PROCEEDINGS OF THE ROYAL SOCIETY A | MATHEMATICAL, PHYSICAL & ENGINEERING SCIENCES

On Local Isotropy of Passive Scalars in Turbulent Shear Flows

K. R. Sreenivasan

Proc. R. Soc. Lond. A 1991 **434**, 165-182
doi: 10.1098/rspa.1991.0087

On local isotropy of passive scalars in turbulent shear flows

By K. R. Sreenivasan
Mason Laboratory, Yale University, New Haven, Connecticut 06520, U.S.A.

[Plate 1]

An assessment of local isotropy and universality in high-Reynolds-number turbulent flows is presented. The emphasis is on the behaviour of passive scalar fields advected by turbulence, but a brief review of the relevant facts is given for the turbulent motion itself. Experiments suggest that local isotropy is not a natural concept for scalars in shear flows, except, perhaps, at such extreme Reynolds numbers that are of no practical relevance on Earth. Yet some type of scaling exists even at moderate Reynolds numbers. The relation between these two observations is a theme of this paper.

1. Introduction

Kolmogorov's (1941) similarity theory introduced the concept that small scales of motion in high-Reynolds-number turbulence are statistically homogeneous, isotropic and universal, and led to certain quantitative predictions. Kolmogorov's original paper, about four pages long, has been enormously influential even in fields besides turbulence. There have been modifications of the original ideas, some by Kolmogorov (1962) himself, but the broad expectation has always remained that some type of universality prevails at small scales. It is also believed that the same basic ideas can be extended to scalar fields advected by turbulence, and that the universal behaviour of the small-scale velocity field would manifest 'naturally' in the scalar field (see Obukhov 1949; Corrsin 1951; Batchelor 1956; Monin & Yaglom 1971). The purpose of this paper is to examine the degree to which local isotropy and universality apply to scalar fields.

Specifically, the problem is this: consider a high-Reynolds-number turbulent flow in which the motion can be decomposed without ambiguity into a time average (or the 'mean') and the superimposed turbulent fluctuation. The turbulent jet sketched in figure 1 provides an example. The mean flow is taken to possess a strong spatial variation, or shear, in one direction, say y; this is also the direction of inhomogeneity in the turbulence structure. Into such a flow inject a scalar, for simplicity, at a length scale comparable with that of the energy-containing motion of turbulence. A measure of this latter scale (designated as L here) is the correlation, or 'integral', length scale. We assume that the scalar is passive in that the turbulence dynamics is not influenced by its presence. Low levels of heating or small doses of a dye injected into the flow provide two examples. The scalar field established under such circumstances will have a mean field (with a non-zero average spatial gradient in the direction y) and a fluctuation field. The questions we seek to address are: At high Reynolds numbers, what are the scaling properties of the fluctuating scalar field at

Proc. R. Soc. Lond. A (1991), **434**, 165–182
Printed in Great Britain

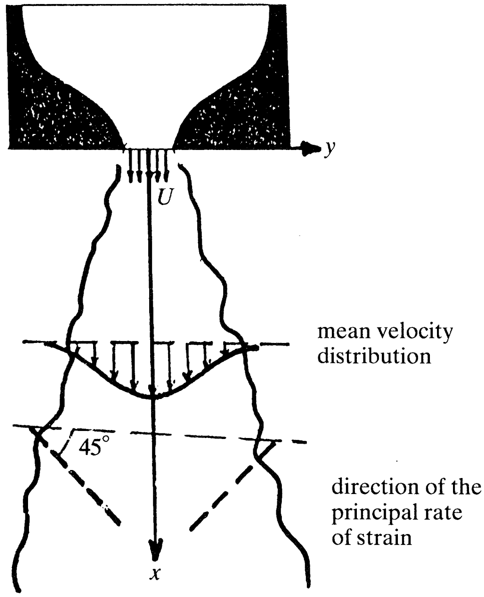

Figure 1. Schematic of a turbulent jet (for example, water jet flowing into water) and the coordinate axes. The outer boundary roughly reflects the average growth of the jet. Typical mean velocity distribution and directions of the principal strain rates in the jet are shown.

scales much smaller than the injection scale? Are there any properties of the scalar field which are universal, in the sense that they do not depend on details of the manner of injection of turbulent energy and of the scalar itself?

These questions have been addressed before, but this paper emphasizes certain features that do not seem to have been appreciated well enough previously. As a background, we present in §2 the spirit of universality of the small-scale turbulent motion itself. We then examine in §3 the strength of the arguments linking universality of small-scale turbulent motion to that of an advected passive scalar, and assess the relevant experimental evidence. There is a final discussion in §4 where principal conclusions are restated.

2. Universality of the small-scale motion of turbulence: a brief review

(a) *The hypothesis and the experimental evidence*

The basic notion underlying Kolmogorov's hypothesis is that of local isotropy, which implies that turbulence scales small compared to L are statistically homogeneous and isotropic. The first hypothesis states that the multivariate probability distributions of the velocity difference in a direction i, $\Delta u_i = u_i(\boldsymbol{x}) - u_i(\boldsymbol{x}+\boldsymbol{r})$, are functions only of $r \equiv |\boldsymbol{r}|$, the average energy dissipation rate, $\langle\epsilon\rangle$, and the kinematic viscosity, ν, of the fluid. Specifically, the nth-order structure functions have the form

$$\langle|\Delta u_i|^n\rangle = (\langle\epsilon\rangle r)^{n/3} f_n(r/\eta). \tag{2.1}$$

Here, $\eta = (\nu^3/\langle\epsilon\rangle)^{\frac{1}{4}}$ is the Kolmogorov length scale formed out of ν and $\langle\epsilon\rangle$, and the functions f_n are universal; η is on the order of magnitude of the energy dissipation scales. One can also define the Kolmogorov velocity formed out of ν and ϵ as $v = (\nu\langle\epsilon\rangle)^{\frac{1}{4}}$. Note that the local Reynolds number $v\eta/\nu = 1$, which implies that η is of the order of magnitude of the smallest dynamical scale.

The second similarity hypothesis is that, at very high Reynolds numbers, there exists a range of scales $\eta \ll r \ll L$, called the inertial range, in which the structure functions become independent of viscosity; that is, $f_n(\infty) = K_n$, where K_n are universal constants independent of the flow. We then have

$$\langle |\Delta u_i|^n \rangle = K_n(\langle \epsilon \rangle r)^{n/3}. \tag{2.2}$$

Kolmogorov spelled out his hypotheses for the real space, but much of the later dissemination of the hypotheses and speculation on their physical content has occurred via wave-number description (Batchelor 1953; Kraichnan 1959; Leslie 1973). Fourier representation is natural for infinitely extended homogeneous fields, but not necessarily so for inhomogeneous flows where the structure in real space and the scales in Fourier space are only loosely related. However, once we accept the wavenumber description, we can quickly see its advantages: it allows a convenient identification of the scales of motion with Fourier modes: one can conceive of a local energy cascade across wavenumber space and argue that there must be a statistical decoupling of large and small scales; one can estimate that the cascade occurs faster with the decreasing scale size so that, even in the infinite Reynolds number limit, the energy flux across the entire spectrum is accomplished on a time scale of the order of the large-eddy turnover time. There is also the distinction to be made between the energy flux across wave numbers and the energy dissipation rate which is its manifestation at the small-scale end of the cascade. The Fourier-space abstraction of events occurring in real space has thus created a rich folklore of nonlinear physics, but it has also led to some problems; we shall return to them in subsequent sections.

It should be noted that (2.1) and (2.2) arise fundamentally from dimensional arguments and that they stand or fall on the support they derive from experiments. In particular, these arguments neglect, at any scale r in the inertial range, the possible contributions of the fluctuations of ϵ over volumes of larger size. This is the so-called intermittency effect, whose first recognition is usually traced to a comment by Landau (Landau & Lifshitz 1963, p. 126; see also Kolmogorov 1962). Landau's comment referred to possible non-universality because the averaging of ϵ is typically performed over many large scales which are flow-specific. It is occasionally thought (Kraichnan 1990, 1991) that the intermittency of small-scale turbulence is decoupled from the energy dynamics and that Kolmogorov's (1941) universality may be exact for second-order statistics (i.e. $n = 2$). Chorin (1986, 1988) has argued that the five-thirds law without any corrections is consistent with intermittency. This issue needs separate consideration, and will be discussed elsewhere.

Be that as it may, it is now fairly well accepted that the structure functions obey, instead of (2.2), the relation

$$\langle |\Delta u_i|^n \rangle = K_n(\langle \epsilon \rangle r)^{\zeta_N}, \tag{2.3}$$

for $\eta \ll r \ll L$, where $\zeta_n \neq \frac{1}{3}n$ for n large. See figure 2. In assessing these data, serious consideration must be given to the convergence of high-order moments of Δu_i, especially for high Reynolds number flows such as the atmospheric surface layer. The key to an accurate determination of high-order scaling exponents at high Reynolds numbers is the fact that the inertial range is quite extensive (that is, there are many steps in the cascade). One can take advantage of this feature and obtain the exponents reliably (Chhabra & Sreenivasan 1991*a*).

On the whole, it thus appears clear that Kolmogorov's original version needs modification. The simplest way of incorporating the intermittency corrections is to

Figure 2

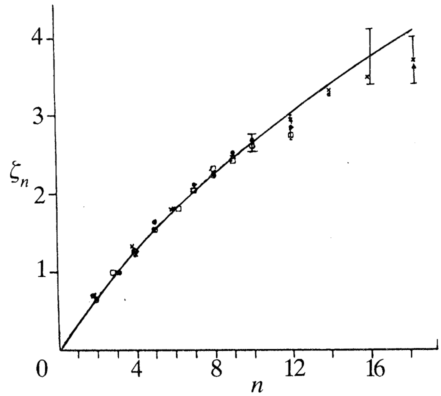

Figure 3

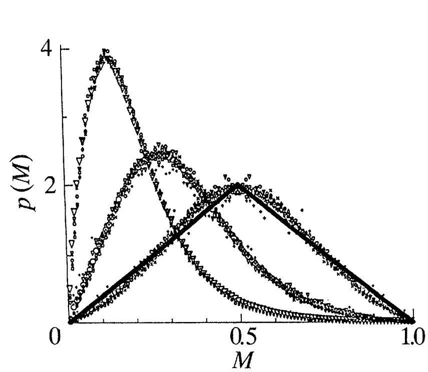

Figure 2. The scaling exponent ζ_n for the velocity structure functions. The symbols are for a turbulent duct flow and a jet, from Anselmet *et al.* (1984). The continuous line is from Chhabra & Sreenivasan (1991*b*) for the atmospheric turbulence.

Figure 3. The probability density $p(M)$ of the multipliers M for the eddy breakdown ratio $m = 2$, 3 and 5 (in order from right to left). These were obtained as follows. A long record of turbulent energy dissipation was obtained by measurement. The total energy flux was calculated by integrating the dissipation over the entire record, and the integral was set to unity. The record was split into two equal parts and the fractions M_1 and M_2 of the energy flux in the two pieces were obtained. The same process was successively repeated by further subdivision of the two pieces. For the nth step, we have 2^n multipliers. The probability density of these multipliers was obtained by considering many such data records. By assuming that there is a direct relation between the breakdown process and this successive averaging procedure, we obtain an insight into the cascade process. Different symbols correspond to different levels of the cascade in the inertial range. The triangular distribution is a simplistic approximation to the binary case ($m = 2$). Data from Chhabra & Sreenivasan (1991*b*).

state formally (Barenblatt 1979) that the self-similarity on the variable r/L is incomplete, and assume (without serious justification) that the functions $f_n(r/\eta, r/L)$ in (2.1) tend to $K_n(r/L)^{-\mu_n}$ as $r/L \rightarrow \infty$ and $r/\eta \rightarrow 0$, where μ_n are undetermined constants presumed to be 'universal' in the sense of being independent of the flow and the scale. This immediately yields (2.3).

Figure 2 encourages the belief that, independent of the modifications required, some sort of universality may prevail in the inertial range dynamics (because the ζ_n are independent of the flow). It is clear that turbulence dynamics in real space must involve vortex-stretching and folding in three dimensions, and all useful modifications of Kolmogorov universality should abstract this feature adequately. Most existing models invoke a cascade of some sort, and bear little resemblance to vortex stretching. Also, universality is not *a priori* guaranteed because vortex stretching even at small scales might involve the large scale, especially in shear flows. Yet phenomenological models (Kolmogorov 1962; Obukhov 1962; Yaglom 1966; Mandelbrot 1974; Frisch *et al.* 1978; Schertzer & Lovejoy 1984; Meneveau & Sreenivasan 1987) based on universality and the concept of cascades may contain certain important elements of the inertial-range physics. One representation of the cascade models is given below.

(*b*) *Cascades and scaling exponents*

At present, there is no means of verifying a cascade picture by directly measuring the scale-to-scale energy transfer rate or flux in the inertial range but some evidence, relevant to the real space, can be given if we assume that the scaling properties of the energy flux at any desired scale r are the same as those of energy dissipation rate averaged over r. This is not completely correct, but probably adequate for considerations of the type discussed below. Assume further that at each cascade step a parent eddy fragments into m subeddies among which the energy flux is divided unevenly, and further that the process of fragmentation and uneven divisions continues until viscous effects are encountered. There is in general no reason to expect that any given step of the cascade will repeat the previous one in detail, but if statistical similarity exists, it should be recognizable as an invariance in the fragmentation process. We proceed as follows. A long record of energy dissipation is obtained from measurement. The total energy flux over the duration of the record is calculated by integrating the dissipation rate ϵ over the record length, and is set to unity. The record is split into m equal parts and the fractions $M_1, M_2, \ldots, M_m$ of the energy flux are obtained; for obvious reasons, we shall call the M_is the multipliers. The number of subeddies (by which we mean m) could vary from one step to the next but, for now, assume that m is independent of the step. We repeat the process of subdivision and obtain the multipliers at each stage. For the nth step, we have m^n multipliers. The probability density of the multipliers can be obtained by considering many such data records. The distributions given in figure 3 were obtained from atmospheric data (Chhabra & Sreenivasan 1991*b*) by assuming, in turn, that $m = 2$, 3 and 5. Different symbols for each m represent different levels of the cascade in the inertial range. The fact that for each m these distributions are nearly identical at different levels suggests, within the framework of assumptions used, the existence of a self-similar process in energy flux. The situation is similar for other flows in the inertial range.

From any one of these distributions, it is possible to obtain the more familiar scaling exponents, for example the ζ_n and the multifractal scaling exponents (Mandelbrot 1974; Hentschel & Procaccia 1983; Frisch & Parisi 1985; Halsey *et al.* 1986; Mandelbrot 1989). Recall that if $E_i(r)$ is the amount of dissipation in a box of size r centred around $\boldsymbol{x}$, then one can decompose the spatial distribution of energy dissipation into interwoven sets of singularity strength α (where $E_i(r) \sim r^{\alpha(x)}$) whose fractal dimension is f(α) (defined according to the relation $N(r) \sim r^{-f(\alpha)}$ where $N(r)$ is the number of boxes containing singularities of strength α). When averaged over a large number of samples, it is more appropriate to define the averages $\langle\alpha\rangle$ and $\langle f(\alpha)\rangle$ of α and $f(\alpha)$ respectively; the averages are related to the exponents $\langle\tau(q)\rangle$ defined by $\Sigma E_i(q) \sim r^{\langle\tau(q)\rangle}$, which are determined by the multiplier distribution (Mandelbrot 1989; Chhabra & Sreenivasan 1991*c*). In one dimension, we have

$$\langle\tau(q)\rangle = \log_m \langle M^q\rangle, \tag{2.4}$$

$$\langle\alpha(q)\rangle = \partial\langle\tau(q)\rangle/\partial q, \tag{2.5}$$

$$\langle f(\alpha)\rangle = q\langle\alpha(q)\rangle - \langle\tau(q)\rangle. \tag{2.6}$$

It is easy to show (Meneveau & Sreenivasan 1991) that the scaling exponents ζ_n are given by

$$\zeta_n = \langle\tau\rangle_{n/3} + 1. \tag{2.7}$$

The exponents ζ_n obtained via the multiplier distributions of figure 3 agree well with

PROCEEDINGS OF THE ROYAL SOCIETY A MATHEMATICAL, PHYSICAL & ENGINEERING SCIENCES

the measured data of Anselmet *et al.* (1984), as shown already in figure 2 for $m = 2$. In fact, $p(M)$ for $m = 2$ can be approximated by a bilinear distribution shown in figure 3. This simple approximation is adequate for most purposes; in particular, the ζ_n so obtained agree well with measurement. Even simpler, and equally effective, approximations to $p(M)$ are possible but will not be discussed here.

From this point of view, one may understand the sample-to-sample fluctuations in $\tau(q)$ or f and α (Meneveau & Sreenivasan 1991; Chhabra & Sreenivasan 1991*b*) as follows. Any single realization will not sample the entire probability space characterized by the miltiplier distributions of figure 3, thus resulting in fluctuations. Chhabra & Sreenivasan (1991*b*) have shown empirically that the fluctuations in f and α are correlated.

We remarked earlier than m could depend on the cascade step. The scaling exponents ζ_n are insensitive to this detail (Chhabra & Sreenivasan 1991*b*), precisely because turbulence does not appear to prefer a special rule for scale-to-scale fragmentation. The $f(\alpha)$ curve obtained by all the $p(M)$s of figure 3 agree, to within reason, with each other.

(*c*) *Local isotropy*

At least at the level of second-order statistics, the evidence (see Monin & Yaglom 1971) in favour of Kolmogorov's hypothesis is considered so solid that it is often forgotten that there is room for worry. Note that all measurements of figure 2 invoke Taylor's hypothesis, namely $r = \Delta t \cdot \langle U \rangle$, where Δt is a time increment in a temporal signal measured by a point probe and $\langle U \rangle$ is the local mean velocity in the direction of the main stream, and that (2.3) has not been subject to rigorous tests of local isotropy. Conclusions from second-order statistics, for which data are available, are not comforting. For example, local isotropy implies that

$$E_v(\kappa_x) = E_w(\kappa_x) = \tfrac{1}{2}[E_u(\kappa_x) - \kappa_x \, \partial E_u(\kappa_x)/\partial \kappa_x], \tag{2.8}$$

where the suffixes u, v and w refer, respectively, to the spectral densities of fluctuations in directions x, y and z; see figure 1. κ_x is the component of the wavenumber in the direction x. The most detailed test of (2.8) appears to have been made by Champagne (1978), who states that the computed spectra $E_v(\kappa_x)$ and $E_w(\kappa_x)$ are in fair agreement with experiment, though consistently higher in the dissipative wavenumber region. This is not an overwhelming endorsement. The few existing measurements of $E_v(\kappa_x)$ and $E_w(\kappa_x)$ – for example Laufer (1954) in the pipe flow, Klebanoff (1955) and Mestayer (1982) in the boundary layer, Kistler & Vrebalovich (1966) in grid turbulence – show hardly any $\frac{5}{3}$ region, and almost all of them are unsupportive of the result from local isotropy that the ratios $3E_v(\kappa_x)/4E_u(\kappa_x)$ and $3E_w(\kappa_x)/4E_v(\kappa_x)$ should be unity in the inertial range (see figure 4). The Reynolds numbers in most of these flows have been thought to be respectably high.

These lapses of local isotropy have been voiced before (Saffman 1968; Kraichnan 1974; Nelkin 1989). If they are real, they deserve serious attention; if they are due to experimental artefacts, they deserve to be set right immediately. The prevailing suspense simply stymies progress.

(*d*) *Summary*

While there is a rough collapse of spectra in the dissipative region (Monin & Yaglom 1971) accurate measurements at high enough wavenumbers do not exist, and so one cannot be definitive about universality even for second-order statistics. In fact, it is not hard to argue that the non-universal effects of intermittency must

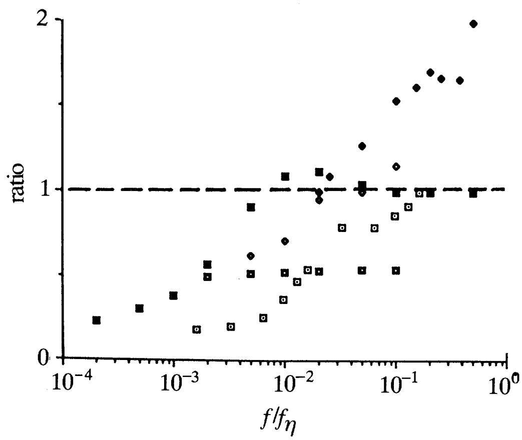

Figure 4. Test for local isotropy in the inertial range. The abscissa is the spectral frequency divided by the Kolmogorov value. The ordinate is the energy ratio described in the text which should be unity in the inertial range. ◆, pipe flow, $R_\lambda = 450$ (Laufer 1954); ⊡, boundary layer, $R_\lambda = 171$ (Klebanoff 1955); □, ◇ grid turbulence, $R_\lambda = 520$ and 670 respectively (Kistler & Vrebalovich 1966); ■, boundary layer, $R_\lambda = 616$ (Mestayer 1982). Since the Reynolds number in all but one of these experiments are comparable, the inertial range is also comparable; as a rough guide, the $\frac{5}{3}$ region in $E_u(\kappa_x)$ lies in the range $3\times10^{-3} < f/f_\eta < 0.1$. Instead of being unity, the energy ratios show no consistent behaviour. There are various concerns that one can express about some of these data, but the point is that an important concept such as local isotropy deserves better validation.

influence the dissipation range; nor is it hard to model these effects in some fashion. The elegance of Kolmogorov's original ideas, which implied a single universal exponent, is lost: instead, we are led to hypothesize an infinity of exponents for which there are no compelling theories. On the bright side, there are reasons to think that some degree of universality prevails in the inertial range dynamics. Even though the connection between the physics of vortex stretching and folding on the one hand and the mechanics of cascades on the other remains very vague, experiments permit the belief that the notion of cascades may usefully abstract the scale-invariant process presumed to occur in the inertial range.

Local isotropy appears a doubtful proposition, at least in the inertial range and for most Reynolds numbers of practical interest. This state of affairs does not seem unreasonable. In the cascade picture, the number of cascades, N, is related to the large-scale Reynolds number Re as $N = \frac{3}{4}\log_m(Re)$. Here $Re = \mathscr{U}L/\nu$, $\mathscr{U}$ being a large-scale velocity, for example, $\frac{1}{3}(u^2+v^2+w^2)^{\frac{1}{2}}$, and we have used the relation $Re^{\frac{3}{4}} = L/\eta$. For a binary cascade where $m = 2$, N would be typically of the order 5 for most laboratory flows and of order 10–12 for geophysical turbulence. This is not a large number. For solar convection, this number is on the order 30. (Assuming, somewhat facetiously, that the whole universe is a fluid system containing hydrogen and helium, and taking current estimates for the size and speed of expansion of the universe, one can estimate N to be no more than a few hundreds!)

Since local isotropy is taken for granted in all extensions of the Kolmogorov-type arguments, we wonder whether its absence undermines the notion of universal dynamics as a fundamental concept. In the next section, we shall investigate its empirical status for the scalar field.

3. The advected scalar field

(a) Some a priori considerations

Consider a dye blob introduced into a shear flow. It will be stretched by not only the turbulent motion but also the mean shear (or the large-eddy motion), which is non-universal. The usual argument for dismissing the mean shear effect is that the scalar is primarily influenced by the straining due to the small-scale, universal, turbulent motion. A typical ratio of the rate-of-strain due to small-scale turbulent motion to that due to the mean shear is of the form

$$(\langle \epsilon \rangle / \nu)^{\frac{1}{2}} / (u/L) = Re^{\frac{1}{2}}. \tag{3.1}$$

Here, u/L represents the large-eddy strain rate and $(\langle \epsilon \rangle/\nu)^{\frac{1}{2}} = (v/\eta)$ is the characteristic strain rate of small-scale turbulence. However, the argument ignores the fact that the small-scale turbulence is not space-filling – in fact, the volume occupied by ϵ tends to zero as the Reynolds number goes to infinity (Sreenivasan & Meneveau 1988) – and that it is poorly correlated with the small-scale field (Meneveau *et al*. 1990). Thus, even though turbulent strain rates are on the average much higher than the mean shear, it is the mean shear that is the effective straining agent over most of the flow. That the correlation time of the strain due to small-scale turbulence is small compared with that of the mean shear renders the latter even more effective. (The effect of mean strain must be manifest also on the vorticity field, but the self-interaction is likely to make the effect weaker.)

Another traditional reason for expecting universality of the scalar field is the presumed behaviour of a non-diffusive scalar in an inviscid flow (because we are considering very high Peclet numbers). The scalar field is governed by the equation

$$\partial c/\partial t + \boldsymbol{u} \cdot \nabla c = \mathscr{D} \nabla^2 c, \tag{3.2}$$

where c is the scalar, $\boldsymbol{u}$ is the local fluid velocity and $\mathscr{D}$ is the scalar diffusivity. Zero diffusivity implies that the scalar associated with a fluid particle remains unchanged during its advection. Kelvin's theorem asserts that the circulation along a fluid contour, or integrated vorticity within the contour, also remains constant. This similarity might suggest that the fate of the scalar field is intimately tied to that of the vorticity field with which it is initially associated, and that the two together might share some of the same qualitative properties. However, the effect of small amounts of scalar diffusion is profound even at very high Peclet numbers. This can be seen vividly in terms of the amplitude probability density function of the scalar. Consider a scalar field in homogeneous and isotropic turbulence, introduced at the initial instant in the form of many strips of small width, within which the concentration is uniform, say unity; the probability density of the scalar field will then have two delta functions, one at zero and the other at unity. No matter how complex the velocity field and how much stretching and twisting the scalar strips undergo (along with their associated vortex tubes), the scalar concentration in the absence of diffusion will always remain either zero or unity, and the probability density will remain unchanged. On the other hand, the asymptotic probability distribution of the scalar in such a case is nearly gaussian centred around the average of half (Eswaran & Pope 1988), and this occurs ultimately by the action of diffusion alone. This simply shows that the non-diffusive limit, like the inviscid limit in turbulence, is singular.

Finally, note that the scalar equation (3.2) is linear. The stochasticity of the scalar

PROCEEDINGS OF THE ROYAL SOCIETY A MATHEMATICAL, PHYSICAL & ENGINEERING SCIENCES

field in the eulerian frame is a consequence either of initial conditions or of the stochasticity of the velocity field $\boldsymbol{u}$, which appears as the coefficient of the spatial advection term. It is often believed that non-trivial universality in systems with many degrees of freedom manifests itself because of nonlinearity; from this point of view, it is *a priori* not clear that the small-scale scalar field should be universal. We might therefore say that a necessary condition for the universality of the scalar field is that the velocity field be universal, but it is clearly not sufficient.

(*b*) *The status of the Corrsin–Obukhov theory in the inertial range*

Let θ be the temperature fluctuation. The Corrsin–Obukhov (Corrsin 1951; Obukhov 1949) expression for the spectral density of θ in the inertial range is of the form (assuming unity Prandtl number)

$$E_\theta(\kappa_x) = \beta\langle\epsilon\rangle^{-\frac{1}{3}}\langle\chi\rangle\,\kappa_x^{-\frac{5}{3}}, \tag{3.3}$$

where $\langle\frac{1}{2}\theta^2\rangle = \int E_\theta(\kappa_x)\,\mathrm{d}\kappa_x$ and $\langle\chi\rangle$ is the average rate at which the scalar variance is being smeared by diffusion effects; β is believed to be a universal constant. The theory assumes, in analogy to Kolmogorov's second hypothesis for the velocity field, that the large scales do not affect inertial-range scales except by setting the average energy dissipation rate $\langle\epsilon\rangle$ and the average scalar dissipation rate $\langle\chi\rangle$. As usual, diffusive effects are assumed to be irrelevant for these scales. The rest of the argument is dimensional

Turning to experiment, figure 5 shows a temperature spectral density measured behind a heated circular cylinder. Using Taylor's hypothesis, it can be interpreted as a wavenumber spectrum. The inset shows that there is a sizeable and unmistakable power law with an exponent of about $-\frac{4}{3}$, which is far less steep than the expected $-\frac{5}{3}$. The scaling at the low-wave number end extends to scales substantially larger than L whereas, at best, it should have extended to no more than a fraction of L. True wavenumber spectra, obtained from one-dimensional spatial cuts of the concentration field (Prasad & Sreenivasan 1990*a*), show that these conclusions are not artifacts of Taylor's hypothesis.

Figure 6 shows that the measured spectral exponent approaches $-\frac{5}{3}$ at high enough Reynolds numbers. (No effort towards a comprehensive data collection was made, but no conscious selection has been applied either!) Whether or not the exponent approaches exactly $\frac{5}{3}$ cannot be determined from this type of measurements.

The standard arguments of incomplete similarity proceed by writing on dimensional grounds that

$$E_\theta(\kappa_x) = \langle\epsilon\rangle^{-\frac{1}{3}}\langle\chi\rangle\,\kappa_x^{-\frac{5}{3}}\psi(\kappa_x L, \kappa_x\eta) \tag{3.4}$$

and that the function $\psi \sim \beta_1(\kappa_x L)^{-\gamma}$ as $\kappa_x L \rightarrow \infty$ and $\psi \sim \beta_2(\kappa_x\eta)^{\delta}$ as $(\kappa_x\eta)\rightarrow 0$, where β_1, β_1, γ, and δ are taken to be constants. (Although the ratios κ_x/κ_y, κ_x/κ_z could also be important, the κ_x-spectra are integrations over κ_y and κ_z spaces, and we will therefore not worry about them explicitly.) It follows that

$$E_\theta(\kappa_x) = \beta\langle\epsilon\rangle^{-\frac{1}{3}}\langle\chi\rangle\,\kappa_x^{-\frac{5}{3}}(\kappa_x L)^{-\gamma}(\kappa_x\eta)^{\delta}, \tag{3.5}$$

with $\beta = \beta_1\beta_2$. Alternatively,

$$E_\theta(\kappa_x) = \beta^*\langle\epsilon\rangle^{-\frac{1}{3}}\langle\chi\rangle\,\kappa_x^{-\frac{5}{3}}(\kappa_x L)^{-\gamma+\delta}, \tag{3.6}$$

where $\beta^* = \beta Re^{-3\delta/4}$ is a Reynolds-number-dependent prefactor.

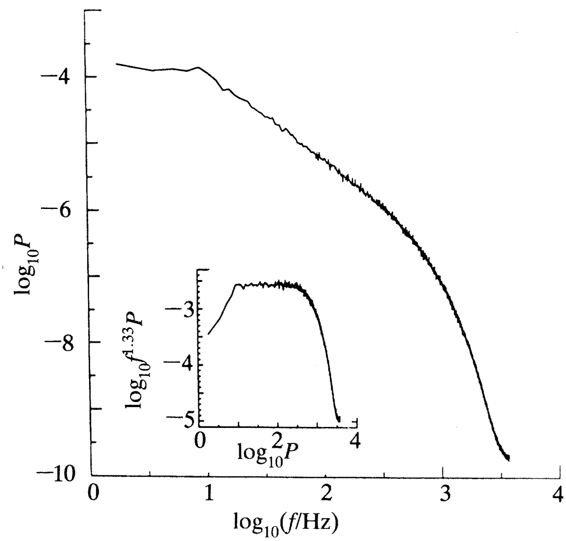

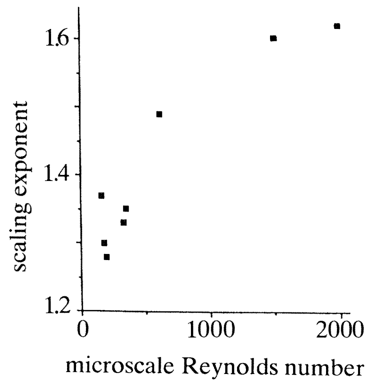

Figure 5. A typical spectral density of temperature fluctuations in the wake of a heated circular cylinder. The oncoming mean air speed was 1770 cm s^{-1}, and the cylinder was 20 mm in diameter. Measurements were made approximately 100 diameters downstream of the cylinder on the wake centreline. At the measurement station, the root-mean-square temperature fluctuation was about 0.36 °C. The inset shows that the slope is close to $\frac{4}{3}$ with about 1.5 decades of scaling.

Figure 6. The variation of the scaling exponent from different sources listed below. Flows considered are the following. Uniform temperature gradient in uniformly sheared turbulence: Tavoularis & Corrsin (1981), spectral slope = 1.28, R_λ = 200–250, scaling range = $10\eta - 2L$ (*ca.* 1.5 decades); wake of a heated cylinder: present measurements, 1.30, 175, $10\eta - 2L$ (*ca.* 1.5 decades); wake of a heated cylinder: present measurements, 1.33, 330, $10\eta - L$ (*ca.* 1.5 decades); wake of a heated cylinder: present measurements, 1.35, 350, $10\eta - 2L$ (*ca.* 1.5 decades); heated boundary layer: Mestayer (1982), 1.49, 616, $10\eta - 2L$ (*ca.* 1.7 decades); atmospheric surface layer: present measurements, 1.6, 1500, $10\eta -$? ? (more than 2 decades); atmospheric surface layer: Pond *et al.* (1966), 1.63, ~ 2000, $10\eta -$? ? (more than 2 decades); dye concentration in wakes (true wavenumber spectra): Prasad & Sreenivasan (1990*a*), 1.37, 160, $2\eta -> L$ (*ca.* 2 decades). It is probably no accident that the scaling exponents in the few measurements of $E_v(\kappa_x)$ fall on the mean curve through the data given here.

That the spectral exponent is a slowly increasing function of the Reynolds number suggests that the asymptotic state is approached slowly (that is, δ is a Reynolds-number-dependent constant). It can be shown, within a cascade picture, that this feature decreases the time required for the scalar variance to be transferred from the large scale to small scale; for the spectral exponent of $-\frac{4}{3}$, this time will be reduced by a factor proportional to $Re^{0.25}$. An implication is that the small scales will have even less time than usual to reach statistical equilibrium. Alternatively, compared with the Corrsin–Obukhov value ($\gamma = \delta = 0$), the scalar variance flux will then accumulate at higher wavenumbers. For $\gamma - \delta = \frac{1}{3}$, the relative rate of accumulation is proportional to $\kappa_x^{\frac{1}{3}}$. The characteristic time for a given scale is then not merely the local eddy-turnover time as is implicit in the Kolmogorov theory, but something larger. This is consistent with diffusion effects influencing 'inertial' timescales of the transfer process.

Even if we restrict attention only to high Reynolds numbers, some non-

Figure 7

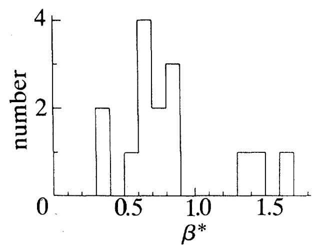

Figure 8

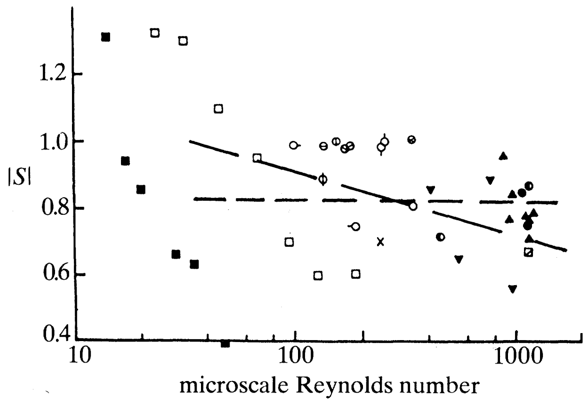

Figure 7. The variation of the constant β^* in (3.6) from different measurements, all of which were made at high Reynolds numbers.

Figure 8. Reynolds number variation of $|S|$ in many shear flows including atmospheric data. The abscissa is the microscale Reynolds number, proportional to $Re^{\frac{1}{2}}$. The left two-thirds or so of the figure were obtained in low and moderate Reynolds number laboratory flows, whereas roughly the right third were obtained in geophysical flows. Different symbols indicate different sources as described in Sreenivasan *et al.* (1979), from where this figure is adapted. Both trends suggested by broken lines are possible. We draw attention to the fact that the ordinate starts at 0.4, not zero.

universality may still manifest itself through the constant β^* in (3.6). According to figure 7, this is a highly variable quantity from one experiment to another even though the Reynolds numbers are all high (when based on the microscale) are within a factor 2. How much of this variability is merely due to inaccurate measurement of $\langle\chi\rangle$ remains unclear.

(*c*) *The status of local isotropy*

In analogy with the velocity gradients, the spatial derivative $\partial\theta/\partial x$ is believed to get its contributions primarily from the high wavenumber part of the spectrum; it is *a priori* not obvious that taking just one derivative of θ ensures the accuracy of the preceeding statement, but there is some empirical evidence (Mestayer 1982) that this is so. If small scales are statistically isotropic, all odd-order moments of this derivative, in particular $\langle(\partial\theta/\partial x)^3\rangle$, must vanish: By reflectional symmetry (a part of the isotropy condition), we should have $\langle(\partial\theta/\partial x)^3\rangle = -\langle(\partial\theta/\partial x)^3\rangle$, so that the derivative skewness $S(=\langle(\partial\theta/\partial x)^3\rangle/\langle(\partial\theta/\partial x)^2\rangle^{\frac{3}{2}})$ must be zero. Measurements, on the other hand, show that $|S|$ is of the order unity (figure 8) even at geophysical Reynolds numbers. These measurements invoke Taylor's frozen flow hypothesis, but it is believed that this will not affect our conclusion seriously. Also, questions raised by Wyngaard (1971) about the velocity sensitivity of the temperature probe have been adequately addressed by Mestayer *et al.* (1976) and Gibson *et al.* (1977). The issue of probe resolution has been examined by Sreenivasan *et al.* (1977) and Mestayer (1982). It is unfortunate that the measurements possess much scatter, and that figure 8 can be interpreted either as having an asymptotic value of about 0.8 independent of Reynolds number, or as showing a weak trend towards zero at some very high Reynolds number. In the former case, local isotropy is violated outright; in the latter case, all reasonable extrapolations of the data suggest that $|S|$ does not attain the expected zero value at any Reynolds number relevant to Earth; only turbulence manifest in heavenly bodies such as the Sun and other stars may possess such high Reynolds numbers! Our intention is not to convey that this conclusion is unshakable, but that it is forced by the existing measurements. Clearly, a result of this importance deserves to be based on more satisfactory data obtained in better-controlled circumstances.

One other point is highly relevant. The derivative skewness is non-zero in homogeneous as well inhomogeneous shear flows. To learn more about the dependence of S on the shear, measurements were made in several slightly heated homogeneous turbulent flows (Sreenivasan & Tavoularis 1980). Several different values of the mean shear, mean temperature gradients, and the relative signs of the two gradients were used in combination. It was found that S vanished only when the mean shear and the mean temperature gradient were both zero or close to it. In all other cases, it was found that:

(*a*) $\operatorname{sgn} S = -\operatorname{sgn}(\mathrm{d}\langle U\rangle/\mathrm{d}y)\operatorname{sgn}(\mathrm{d}\langle T\rangle/\mathrm{d}y)$, where $\langle U\rangle$ and $\langle T\rangle$ are the mean velocity and mean temperature respectively (see also Mestayer *et al.* 1976; Gibson *et al.* 1977; Mestayer 1982);

(*b*) $|S|$ varies roughly linearly with the magnitude of $(L/\theta^1)\cdot \mathrm{d}\langle T\rangle/\mathrm{d}y$ for small magnitudes, but becomes independent of it beyond some range;

(*c*) $|S|$ depends on the history of the mean shear $\mathrm{d}\langle U\rangle/\mathrm{d}y$.

We conclude that the quantity S, believed to be a small-scale property of the scalar, is directly linked to the mean shear (or the large-structure). While the Reynolds numbers in these flows were only moderately high, data at higher Reynolds numbers obtained by Mestayer *et al.* (1976), Gibson *et al.* (1977), Mestayer (1982), including some in the atmosphere, are completely consistent with (*a*) above.

Local isotropy also demands the skewness of the derivatives $\partial\theta/\partial y$ and $\partial\theta/\partial z$ to vanish. Measurements (see, for example, Sreenivasan *et al.* 1977) confirm that $\partial\theta/\partial y$ has the same magnitude of skewness as $\partial\theta/\partial x$ (but has the opposite sign), but the two-dimensionality of the mean flow (i.e. homogeneity in the direction z) renders the skewness of $\partial\theta/\partial z$ zero.

Yet another requirement of local isotropy is that the different components of the scalar dissipation $\chi = \mathscr{D}|\operatorname{grad}\theta|^2$ must be equal. Measurements in the boundary layer (Sreenivasan *et al.* 1977) have shown that the ratios of $(\partial\theta/\partial x)^2/(\partial\theta/\partial y)^2$ and $(\partial\theta/\partial x)^2/(\partial\theta/\partial z)^2$ are typically 0.7 and 0.5 respectively. Very nearly the same values were obtained for the concentration field of a dye in a jet (Prasad & Sreenivasan 1990*b*). Lest it be thought that this is a low Reynolds number effect, we should mention that our unpublished temperature measurements in the atmosphere confirm this fact.

Finally, local isotropy is not compelling in the inertial range either. Local isotropy implies certain relations between the κ_x-spectra of $\partial\theta/\partial x$ on the one hand and those of $\partial\theta/\partial y$ and $\partial\theta/\partial z$ on the other (Van Atta 1977). As shown by Van Atta, the measured spectral density (Sreenivasan *et al.* 1977) of $\partial\theta/\partial y$ compares poorly with that calculated on the basis of local isotropy and the measured spectral density of $\partial\theta/\partial x$. (A similar comparison for $\partial\theta/\partial z$ is good, this being no surprise because of the strong large-scale z-symmetry in two-dimensional flows.)

Taking the available measurements on their face value, we should ask: Why this lack of local isotropy? It is easy to see that the scalar field in the presence of mean shear is not isotropic in detail. From a planar cut through the dye concentration field in a turbulent jet, one can obtain the dissipative structure $\mathscr{D}|\operatorname{grad} c|^2$. The many

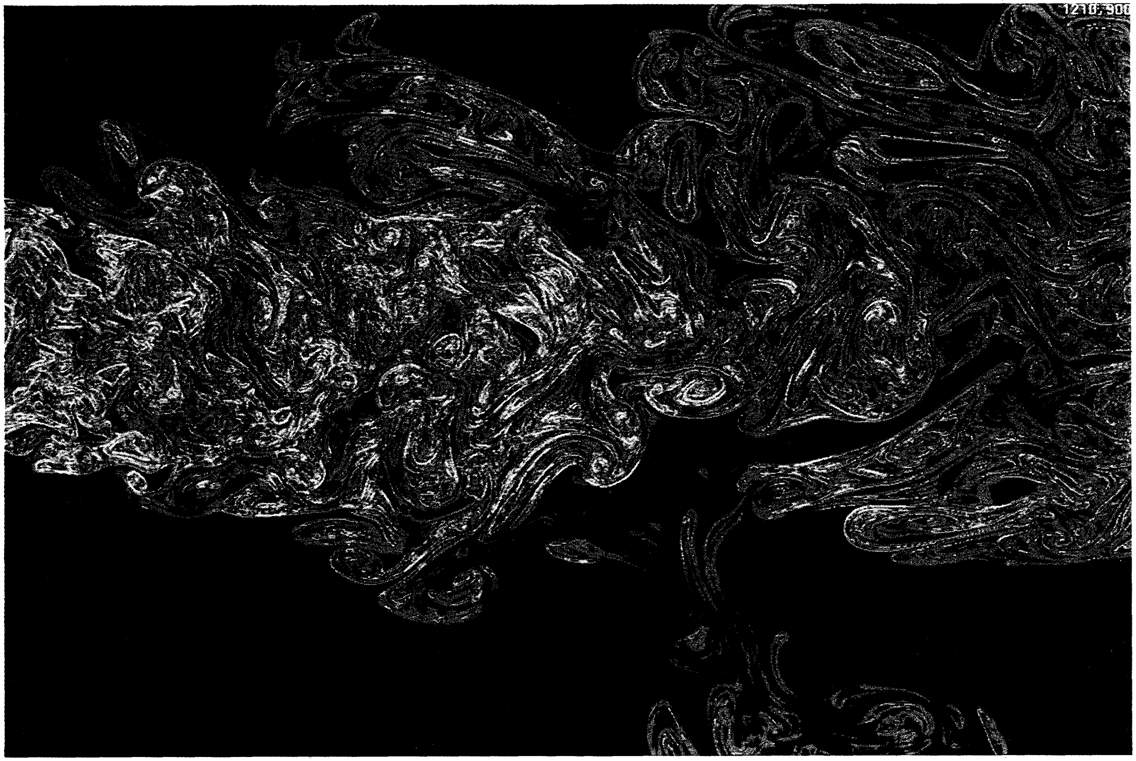

Figure 9. A two-dimensional image of an axisymmetric water jet was obtained by the laser induced fluorescence (LIF) technique. A Nd:YAG laser beam shaped into a sheet of 200–250 μm thickness using suitable lenses was directed into a water tank into which the jet fluid was emerging from a well-contoured nozzle and standard upstream flow management; the jet fluid contained small amounts of uniformly dispersed fluorescing dye (sodium fluorescein). The fluorescence excited by the laser radiation was captured on a digital camera (a charge-coupled-device, with a pixel array size of 1300×1035). The pixel intensity in the digital image was linearly related to the concentration of the dye. The laser had a power density of about 2×10^7 J s^{-1} per pulse, and a pulse duration of 10 ns. The flow is thus frozen to an excellent approximation. The region in the image extends from 8 to 24 nozzle diameters. The nozzle Reynolds number was about 4000. The laser sheet thickness was between one and two $<\eta>$, where $<\eta>$ is the Kolmogorov thickness averaged over the image. From the LIF map of the concentration field, c, one can calculate an approximation to the 'dissipation' rate, $\mathscr{D}\,|\text{grad}\, c|^2$, of the variance of concentration fluctuations (resolved only up to scales of the order of $<\eta>$). This is shown in the figure. The gradient of the concentration was approximated by finite differences; only two components of $|\text{grad}\, c^2|$ were calculated. Inclusion of the third component (Prasad & Sreenivasan 1990*b*) does not alter the picture. Different colours represent, in some nonlinear scaling, different magnitudes of the 'dissipation' rate; magnitudes increase from deep blue through red and, finally, white.

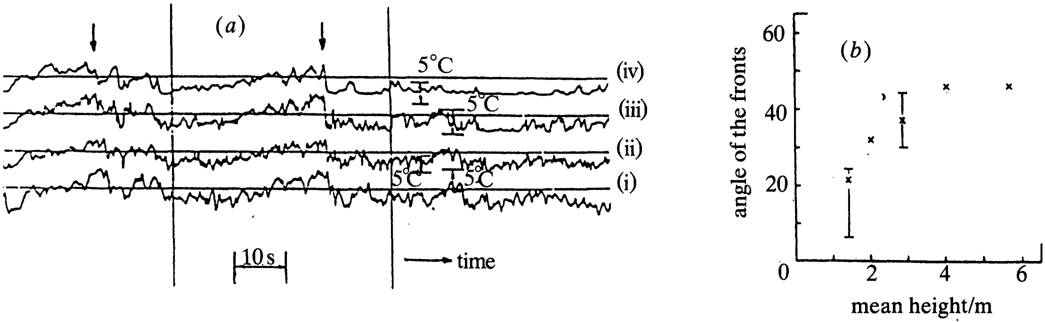

Figure 10. (*a*) Some typical time traces of the temperature fluctuations in the atmosphere, measured by Phong-Anant *et al.* (1990) simultaneously by using four temperature probes at heights of (i) 1, (ii) 2, (iii) 4 and (iv) 8 m above the ground. (The probe at 4 m is 1 m upwind of the others.) Using Taylor's hypothesis, the time traces are equivalent to taking spatial cuts by a fast-moving probe. Arrows indicate two examples of sharp structures extending over several metres of the atmospheric surface layer. Note the characteristic ramp-like features, say between the left vertical line and the second arrow. Their typical lengths in this figure are of the order of 50 m. (*b*) The angle of inclination of the temperature ramps estimated directly from the height difference between any two probes, the wind velocity at an average height between them, and the relative time difference of arrival of the fronts at those heights. The angle is plotted against the geometric mean of the two heights in question. Estimates based on a different statistical method yield nearly the same results. More extensive temperature measurements made in a moderate-Reynolds-number, slightly heated, laboratory boundary layer (Chen & Blackwelder 1978) are also consistent with the present picture.

elongated structures in figure 9, plate 1, represent sheet-like objects in three dimensions; limited three-dimensional measurements (Prasad & Sreenivasan 1990*b*) verify this premise. Although the precise shape of these sheet-like structures depends moderately on the definition used to identify them, some of their statistical properties can be quantified reliably (Prasad & Sreenivasan 1988, 1990*b*); in any case, it is clear that their size in one direction is quite commonly on the order of the large scale L though small in the perpendicular direction. Their sizes in the third direction are in-between. (It is thus more sensible to designate them as thin structures rather than small scales but, for convenience, we shall occasionally use the standard terminology.) The dye structure in the far-field of a turbulent wake (cylinder Reynolds number of 1500) shares the same features.

The presence of stretched structures does not in itself negate statistical isotropy but the point is that, away from the jet axis, the elongated structures have a preferential orientation. These structures have finite lifetimes but new ones, similarly oriented, are born continuously. From a number of observations, it appears that their predominant orientation is about 45° to the mean flow. It is probably no accident that 45° is the principal axis for a two-dimensional mean strain field. It is also known that the smoke injected into the outer part of a turbulent boundary layer arranged itself into structures aligned in the 45° direction (Head & Bandyopadhyay 1981). Finally, this view seems consistent with the structures near the jet axis being nearly horizontal in figure 9 because of the global symmetry (see figure 1).

The rough notion could thus be put forth that statistical isotropy is not 'natural' or 'obvious' for the small-scale scalar field in a shear flow. We are aware that the flow Reynolds number in these examples is not very high, and so turn to the temperature field in atmospheric turbulence whose large-scale Reynolds number is three to four orders of magnitude higher. Unfortunately, we do not have the same detailed picture

PROCEEDINGS OF THE ROYAL SOCIETY A MATHEMATICAL, PHYSICAL & ENGINEERING SCIENCES

for the atmosphere, but there do exist (Phong-Anant *et al.* 1990) temperature traces obtained at several heights by means of point probes; see also Antonia *et al.* (1979). The traces show the prevalence of characteristic 'ramp-like' large structure extending in a coherent fashion for many metres (figure 10*a*), with their fronts oriented at approximately 45° to the mean flow (figure 10*b*). (Very near the ground, the angle is smaller perhaps because of the direct effect of the ground.) By observing the similarity between the ramp-like occurrences in the concentration field with the stretched structures of figure 9, we tentatively conclude that the two have the same source. These 'fronts' would then correspond to the thin structures mentioned earlier, and are intimately related to large-scale features (in a manner reminiscent of the long-time solution to Burgers equation).

Mention may also be made of the demonstration of Sreenivasan *et al.* (1979) that most of the contribution to the non-zero value of S comes from ramp-like structures.

(*d*) *Higher-order statistics*

Similar to the scaling of velocity structure-functions, one may conceive of scaling exponents for the temperature structure functions. Such measurements (Antonia *et al.* 1984), including some of our own, are not as definitive as the velocity structure functions. At present, we cannot conclude much about universality.

4. Discussion and conclusions

The following summary remarks may be useful.

1. The asymptotic state of the scalar field is reached very slowly in Reynolds numbers. For most Reynolds numbers, diffusive effects seem important even in the 'inertial range'. There is hardly any credible evidence that this asymptotic state is unique.

2. If local isotropy seemed somewhat dubious for the velocity field, it seems even more so for the scalar field. Existing measurements suggest that local isotropy is not attained in the dissipation range, except perhaps at such extremely large Reynolds numbers as to be of no consequence in practice. While the evidence in the 'inertial range' is less unequivocal, the situation is qualitatively the same.

3. The small-scale scalar field has a tendency to form well-defined 'structure' in the real space, and it is an integral part of the large structure (as in temperature ramps). Structures of disparate scales directly interact with each other without several intermediate steps.

4. The predominant mechanism responsible for the elongated structures appears to be the mean or large-eddy strain-rate over a large part of the volume occupied by the scalar, probably precluding universality. The average description of the eddy breakdown – if the stretching and folding effect can be called that – is quite unlike the cascade picture usually visualized in Kolmogorov-type scenarios.

Given these, should we presume that the arguments rooted in Kolmogorov are basically sound and spend our efforts at 'modifying' them (as was exemplified in §3*b*)? Or, should we discard the familiar ground altogether and look for alternatives more faithful to the observed structure? How can we model the interaction of structures at different scales? How do we explain the respectable scaling observed at moderate Reynolds numbers? Why exactly is the spectral exponent close to $\frac{5}{3}$ at high Reynolds numbers? What are the minimum conditions under which the $\frac{5}{3}$ law can be observed? What is the correspondence between the structure in the physical space and the scale in the wavenumber space? An effort at fully understanding these issues will be clearly well spent.

Kraichnan (1974) considered the possibility that the so-called inertial range is merely the upper end of the spectra of coherent thin structures, but himself argued against it for the velocity field. We speculate that Kraichnan's arguments may be less valid for the scalar field. If this is so, the Kolmogorov framework will be incidental to the observed scaling.

A different view is that the localness of wavenumber interaction is not inconsistent with the fact that the thin structure is strongly coupled to the large structure in physical space, and that the Kolmogorov framework is a sound approximation. A case in point is the solution to Burgers equation which is of the sawtooth type, not very different from the ramp structures of figure 10*a*. For such structures, Kraichnan (1974) has shown that the non-local transfer of energy from small wavenumbers to large wavenumbers is small at any given instant of time; however, when integrated over long times, the non-local interaction could add up to be large. Kolmogorov-type arguments merely demand that the non-local transfer be small at any given instant of time. It is therefore conceivable that the highly stretched objects, which are the result of an integrated effect, do not negate local energy transfer in wavenumber space. On the other hand, Kraichnan has also reminded us that this localness of interaction is merely a reflection of the spectral roll-off rate, and may not have much physical content to it. We tentatively conclude that the observed spectral scaling should not necessarily force us into blindly accepting the physical content of Kolmogorov-type cascades for the scalar field.

An interesting argument in this connection (Chorin 1990) is that the $-\frac{5}{3}$ law is no more than a reflection of global conservation properties obeyed by a three-dimensional stochastic field. Chorin advances this possibility on the basis of his simulations of vortex filaments executing random walks according to a set of stochastic rules. As pointed out by Chorin himself, there are many unresolved issues about the relevance of these calculations to Navier–Stokes turbulence but, in itself, it is interesting that some statistical mechanical system close to equilibrium should have the scaling exponent of $\frac{5}{3}$. Chorin's claim has certain attractiveness to it and deserves further study.

We now come to the final point. Whatever alternatives one proposes, it seems to us that they should remain as true as possible to events in physical space, and incorporate the observed structure. How exactly this should be done remains unclear, but the heart of the matter is the relation between the structure in real space and the scale in the wavenumber space. Fourier decomposition is not a versatile enough vehicle for the purpose, but the alternatives do not seem too compelling at present; this is so in spite of the recent application to turbulence of orthonormal basis functions such as wavelets (Argoul *et al.* 1989; Everson *et al.* 1990; Farge *et al.* 1990) and wavelet-packets (Zubair *et al.* 1991) where the notions of scale and structure are separately handled.

Most alternative suggestions are likely to be anticlimactic, but consider the following tentative model which treats the structure and scale separately. The model attempts to determine an average real-space transformation according to which a structure at one scale breaks down to substructures at a smaller scale. We use a wavelet decomposition and assume that, by this means, the structures at various scales can be identified. This analysis (Everson *et al.* 1990) shows that the large structures are blob-like whereas the smaller ones look more and more string-like (in two-dimensional sections); at the finest scale resolved, the structures resemble those in figure 9, as expected. One can now conceive of a simple affine mapping to model the transformation of structures from one scale to another.

The transformation is obtained as follows. Let us identify the structures by a simple scheme (involving contour identification) and count their number for each wavelet scale. For the jet, the data show that this number increases by a factor of 2.6 whenever the scale decreases by factor 2. The number 2.6 is quite robust in the scale range between $2L$ and a few η, and indicates that the division of a large structure into smaller ones does not occur on the average in a binary fashion (which, in two dimensions, would have increased the number of structures fourfold for a scale reduction by 2). It also turns out, to an excellent approximation, that the aspect ratio (that is, the length/thickness ratio) of the structures in the same scale range increases by a factor of about 2 for each reduction in scale size by a factor 2.

Now for some speculation: if the fact that 2.6 is almost exactly equal to the square of the golden mean is more than a happenstance in this case, we can make the following model. At each stage of scale refinement by a factor 2, the generation of new scales follows a golden mean rule; that is, the number of substructures in one dimension increases according to the Fibonacci sequence 1, 2, 3, 5, 8, 13, ... As is well known, the ratio of succeeding numbers in this sequence converges to the golden mean. This implies that, on the average one structure breaks down into two substructures while, at the next stage, one of the substructures remains unchanged whereas the other breaks down into two, and so on.

It remains for us to determine the rule according to which the scalar variance associated with a structure gets split among its offsprings. At any scale, if the structure that breaks down splits the scalar variance in the ratio 0.87/0.13, all the measured scaling exponents such as those described in §2*b* can be duplicated quite accurately. This is an invariant ratio in the scale range already mentioned.

The chief merit of this effort is probably that it explicitly recognizes the structures at various scales; new and more far-reaching ideas along these lines are much needed.

I have benefited greatly from discussions over a period of time with Ira Bernstein, Michael Fisher, Robert Kraichnan, Benoit Mandelbrot, Mark Nelkin, Philippe Similon and Larry Sirovich. The typescript was carefully read by David Kyle, Juan de la Mora, Charles Meneveau, Mark Nelkin, Philippe Similon and Anil Suri. Figures 3, 5 and 9 were obtained in collaboration with Ashvin Chhabra, Rahul Prasad and Purushothaman Kailasnath. To them all, I am grateful. The work was financially supported by AFOSR and DARPA.

References

Argoul, F., Arneodo, A., Grasseau, G., Cagne, Y., Hopfinger, E. J. & Frisch, U. 1989 *Nature, Lond.* **338**, 51–53.

Anselmet, F., Gagne, Y., Hopfinger, E. J. & Antonia, R. A. 1984 *J. Fluid Mech.* **140**, 63–89.

Antonia, R. A., Chambers, A. J., Friehe, C. A. & Van Atta, C. W. 1979 *J. atmos. Sci.* **36**, 99–108.

Antonia, R. A., Hopfinger, E. J., Gagne, Y. & Anselmet, F. 1984 *Phys. Rev.* A **30**, 2704–2707.

Barenblatt, G. I. 1979 *Similarity, self-similarity, and intermediate asymptotics.* Consultants Bureau.

Batchelor, G. K. 1953 *The theory of homogeneous turbulence.* Cambridge University Press.

Batchelor, G. K. 1956 *J. Fluid Mech.* **5**, 113–133.

Champagne, F. H. 1978 *J. Fluid Mech.* **86**, 67–108.

Chen, C.-H.P. & Blackwelder, R. F. 1978 *J. Fluid Mech.* **89**, 1–31.

Chhabra, A. B. & Sreenivasan, K. R. 1991*a* In *New perspectives in turbulence* (ed. L. Sirovich). Springer.

Chhabra, A. B. & Sreenivasan, K. R. 1991*b* (In the press.)

Chhabra, A. B. & Sreenivasan, K. R. 1991*c* *Phys. Rev.* A **43**, 1114–1117.

Chorin, A. J. 1986 *Communs pure appl. Math.* **39**, s47–s65. (Special issue.)

Chorin, A. J. 1988 *Phys. Rev. Lett.* **60**, 1947–1949.

Chorin, A. J. 1990 *Communs math. Phys.* **132**, 519–536.

Corrsin, S. 1951 *J. appl. Phys.* **22**, 469–473.

Eswaran, V. & Pope, S. B. 1958 *Phys. Fluids* **31**, 506–520.

Everson, R., Sirovich, L. & Sreenivasan, K. R. 1990 *Phys. Lett.* A **145**, 314–322.

Farge, M., Guezennec, Y., Ho, C. M. & Meneveau, C. 1990 In *Proc. Summer Prog. Center for Turbulence Research*. NASA-Ames and Stanford.

Frisch, U. & Parisi, G. 1985 In *Turbulence and predictability in geophysical fluid dynamics* (ed. M. Ghil, R. Benzi & G. Parisi), pp. 84–88. North-Holland.

Frisch, U., Sulem, P.-L. & Nelkin, M. 1978 *J. Fluid Mech.* **87**, 719–736.

Gibson, C. H., Friehe, C. A. & McConnel, S. O. 1977 *Phys. Fluids Suppl.* **20**, s156–s157.

Halsey, T. C., Jensen, M. H., Kadanoff, L. P., Procaccia, I. & Shraiman, B. 1986 *Phys. Rev.* A **34**, 3325–3340.

Head, M. R. & Bandyopadhyay, P. R. 1981 *J. Fluid Mech.* **107**, 297–338.

Hentschel, H. G. E. & Procaccia, I. 1983 *Physica* D **8**, 435–444.

Kolmogorov, A. N. 1941 *C.r. Acad. Sci. USSR* **30**, 299–303. (English translations of Kolmogorov's (1941) papers can be found in *Turbulence: classical papers on statistical theory* (ed. S. K. Friedlander & L. Topper), pp. 151–160. Interscience (1961).)

Kolmogorov, A. N. 1962 *J. Fluid Mech.* **13**, 82–85.

Kistler, A. L. & Vrebalovich, T. 1966 *J. Fluid Mech.* **26**, 37–47.

Klebanoff, P. S. 1955 *NACA Rep.* 1247.

Kraichnan, R. H. 1959 *J. Fluid Mech.* **5**, 497–543.

Kraichnan, R. H. 1974 *J. Fluid Mech.* **62**, 305–330.

Kraichnan, R. H. 1990 *Phys. Rev. Lett.* **65**, 578–581.

Kraichnan, R. H. 1991 In *New perspectives in turbulence* (ed. L. Sirovich). Springer.

Laufer, J. 1954 *NACA Rep.* 1174.

Leslie, D. C. 1973 *Developments in the theory of turbulence*. Oxford University Press.

Mandelbrot, B. B. 1974 *J. Fluid Mech.* **62**, 331–358.

Mandelbrot, B. B. 1989 *Pure appl. Geophys.* **131**, 5–42.

Meneveau, C. & Sreenivasan, K. R. 1987 *Phys. Rev. Lett.* **59**, 1424–1427.

Meneveau, C. & Sreenivasan, K. R. 1991 *J. Fluid Mech.* **224**, 429–484.

Meneveau, C., Sreenivasan, K. R., Kailasnath, P. & Fan, M. S. 1990 *Phys. Rev.* A **41**, 894–913.

Mestayer, P. G. 1982 *J. Fluid Mech.* **125**, 475–503.

Mestayer, P. G., Gibson, C. H., Coantic, M. F. & Patel, A. S. 1976 *Phys. Fluids* **19**, 1279–1287.

Monin, A. S. & Yaglom, A. M. 1971 *Statistical fluid mechanics*, vol. 2. MIT Press.

Nelkin, M. 1989 *J. statist. Phys.* **54**, 1–15.

Obukhov, A. M. 1949 *Izv. Akad. Nauk SSSR. Geogr. Geofiz.* **13**, 58–69.

Obukhov, A. M. 1962 *J. Fluid Mech.* **13**, 77–82.

Phong-Anant, D., Antonia, R. A., Chambers, A. J. & Rajagopalan, S. 1990 *J. geophys. Res.* **85**, 424–438.

Pond, S., Smith, S. D., Hamblin, P. F. & Burling, R. W. 1966 *J. atmos. Sci.* **23**, 376–386.

Prasad, R. R. & Sreenivasan, K. R. 1988 *Phys. Rev. Lett.* **61**, 74–77.

Prasad, R. R. & Sreenivasan, K. R. 1990*a* *Phys. Fluids* A **2**, 792–807.

Prasad, R. R. & Sreenivasan, K. R. 1990*b* *J. Fluid Mech.* **216**, 1–34.

Schertzer, D. & Lovejoy, S. 1983 In *Turbulent shear flows 4* (ed. B. Launder *et al.*), pp. 7–33.

Sreenivasan, K. R. & Meneveau, C. 1988 *Phys. Rev.* A **38**, 6287–6295.

Sreenivasan, K. R. & Tavoularis, S. 1980 *J. Fluid Mech.* **101**, 783–795.

Sreenivasan, K. R., Antonia, R. A. & Britz, D. 1979 *J. Fluid Mech.* **94**, 745–775.

Sreenivasan, K. R., Antonia, R. A. & Danh, H. Q. 1977 *Phys. Fluids.* **20**, 1238–1249.

Sreenivasan, K. R., Prasad, R. R., Meneveau, C. & Ramshankar, R. 1989 *Pure appl. Geophys. J.* **131**, 43–60.

Tavoularis, S. & Corrsin, S. 1981 *J. Fluid Mech.* **104**, 311–347.

Van Atta, C. W. 1977 *J. Fluid Mech.* **80**, 609–615.

Wynngard, J. C. 1971 *J. Fluid Mech.* **48**, 763–769.

Yaglom, A. M. 1966 *Soviet Phys. Dokl.* **2**, 26–29.

Zubair, L., Sreenivasan, K. R. & Wickerhauser, V. 1991 In *Perspectives in turbulence* (ed. T. Gadsky, S. Sirkhar & C. G. Speziale). Springer.

Note added in proof (*3 May 1991*). In some recent work (J. Brasseur, *AIAA Paper* 91–0230), the author has argued on the basis of his computations that there is a strong interaction between the large and small scales of the velocity field, and that the anisotropy of small scales is unlikely to vanish even in the infinite Reynolds number limit if the energy-containing scales are anisotropic.

Colour plate printed in Great Britain by George Over Limited, London and Rugby

PROCEEDINGS OF THE ROYAL SOCIETY A MATHEMATICAL, PHYSICAL & ENGINEERING SCIENCES

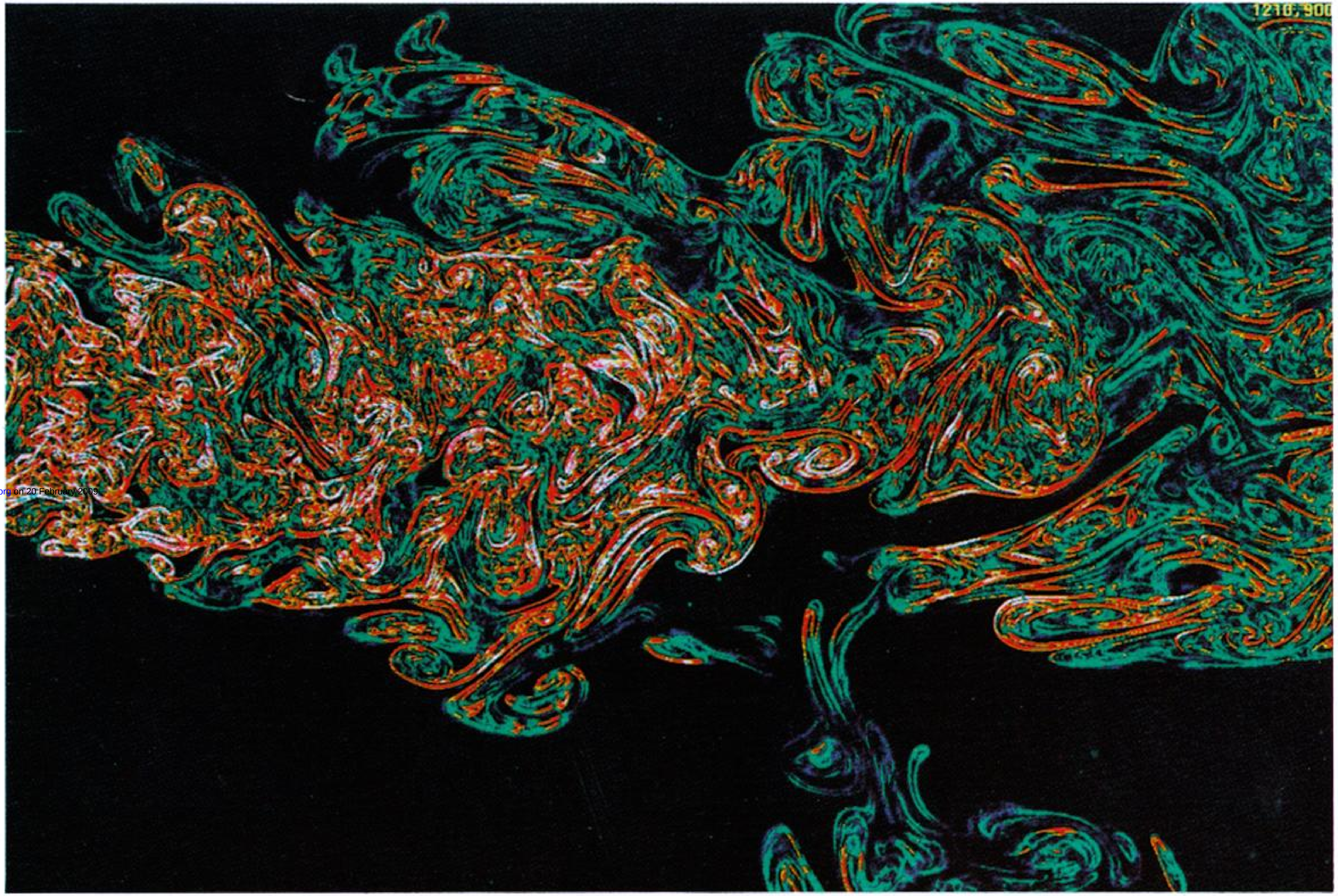

Figure 9. A two-dimensional image of an axisymmetric water jet was obtained by the laser induced fluorescence (LIF) technique. A Nd:YAG laser beam shaped into a sheet of 200–250 μm thickness using suitable lenses was directed into a water tank into which the jet fluid was emerging from a well-contoured nozzle and standard upstream flow management; the jet fluid contained small amounts of uniformly dispersed fluorescing dye (sodium fluorescein). The fluorescence excited by the laser radiation was captured on a digital camera (a charge-coupled-device, with a pixel array size of 1300×1035). The pixel intensity in the digital image was linearly related to the concentration of the dye. The laser had a power density of about 2×10^{7} J s^{-1} per pulse, and a pulse duration of 10 ns. The flow is thus frozen to an excellent approximation. The region in the image extends from 8 to 24 nozzle diameters. The nozzle Reynolds number was about 4000. The laser sheet thickness was between one and two $<\eta>$, where $<\eta>$ is the Kolmogorov thickness averaged over the image. From the LIF map of the concentration field, c, one can calculate an approximation to the 'dissipation' rate, $\mathscr{D}\ |\text{grad}\ c|^2$, of the variance of concentration fluctuations (resolved only up to scales of the order of $<\eta>$). This is shown in the figure. The gradient of the concentration was approximated by finite differences; only two components of $|\text{grad}\ c^2|$ were calculated. Inclusion of the third component (Prasad & Sreenivasan 1990b) does not alter the picture. Different colours represent, in some nonlinear scaling, different magnitudes of the 'dissipation' rate; magnitudes increase from deep blue through red and, finally, white.

PROCEEDINGS OF THE ROYAL SOCIETY A MATHEMATICAL, PHYSICAL & ENGINEERING SCIENCES